ResearchGate

See discussions, stats, and author profiles for this publication at: https://www.researchgate.net/publication/44577187

Core-Shell Diamond as a Support for Solid-Phase Extraction and High-Performance Liquid Chromatography

ARTICLE *in* ANALYTICAL CHEMISTRY · JUNE 2010

Impact Factor: 5.64 · DOI: 10.1021/ac1002068 · Source: PubMed

CITATIONS
29

READS
41

8 AUTHORS, INCLUDING:

David Jensen

78 PUBLICATIONS **253** CITATIONS

SEE PROFILE

Andrew Dadson

US Synthetic

55 PUBLICATIONS **270** CITATIONS

SEE PROFILE

Vaithiyalingam Shutthanandan

Pacific Northwest National Laboratory

251 PUBLICATIONS **4,158** CITATIONS

SEE PROFILE

Matthew R Linford

Brigham Young University - Provo Main Ca…

282 PUBLICATIONS **4,913** CITATIONS

SEE PROFILE

Available from: Matthew R Linford
Retrieved on: 31 January 2016

Anal. Chem. **2010,** *82,* 4448–4456

Core–Shell Diamond as a Support for Solid-Phase Extraction and High-Performance Liquid Chromatography

Gaurav Saini,[†] David S. Jensen,[†] Landon A. Wiest,[†] Michael A. Vail,[‡] Andrew Dadson,[‡] Milton L. Lee,[†] V. Shutthanandan,[§] and Matthew R. Linford*[,†]

Department of Chemistry and Biochemistry, Brigham Young University, Provo, Utah 84602, U.S. Synthetic Corporation, Orem, Utah 84058, and Environmental Molecular Sciences Laboratory, Pacific Northwest National Laboratory, Richland, Washington 99352

We report the formation of core–shell diamond particles for solid-phase extraction (SPE) and high-performance liquid chromatography (HPLC) made by layer-by-layer (LbL) deposition. Their synthesis begins with the amine functionalization of microdiamond by its immersion in an aqueous solution of a primary amine-containing polymer (polyallylamine (PAAm)). The amine-terminated microdiamond is then immersed in an aqueous suspension of nanodiamond, which leads to adsorption of the nanodiamond. Alternating (self-limiting) immersions in the solutions of the amine-containing polymer and the suspension of nanodiamond are continued until the desired number of nanodiamond layers is formed around the microdiamond. Finally, the core–shell particles are cross-linked with 1,2,5,6-diepoxycyclooctane or reacted with 1,2-epoxyoctadecane. Layer-by-layer deposition of PAAm and nanodiamond is also studied on planar Si/SiO_2 surfaces, which were characterized by scanning electron microscopy (SEM), Rutherford backscattering spectrometry (RBS), and nuclear reaction analysis (NRA). Core–shell particles are characterized by diffuse reflectance infrared Fourier transform spectroscopy (DRIFT), environmental scanning electron microscopy (ESEM), and Brunauer–Emmett–Teller (BET) surface area and pore size measurements. Larger (ca. 50 μm) core–shell diamond particles have much higher surface areas and analyte loading capacities in SPE than nonporous solid diamond particles. Smaller (ca. 3 μm), normal and reversed-phase, core–shell diamond particles have been used for HPLC, with 36 300 plates/m for mesitylene in a separation of benzene and alkyl benzenes and 54 800 plates/m for diazinon in a similar separation of two pesticides on a C_{18} adsorbent.

Silica is the dominant support material employed in liquid chromatography (LC), and it is also heavily used in solid-phase extraction (SPE).[1,2] It can be synthesized as highly uniform and spherical particles with controllable porosity, and its surface chemistry is well-understood, allowing straightforward functionalization by silanization.[2] Its disadvantages include the labile nature of the Si–O–Si bond between silane adsorbates and the SiO_2 substrate under acidic conditions, the inherent instability of SiO_2 under basic attack, and the often undesirable acidity of residual silanol groups.[2,3] Both silica and polymeric stationary phases are commonly employed in SPE, where polymeric SPE adsorbents are generally much more stable against acid or base hydrolysis than their silica counterparts.[4] However, polymeric materials appear to be less than optimal supports for LC—if not highly cross-linked they may swell in the presence of organic solvents, they tend to have low mechanical strengths, and they often suffer from poor efficiencies.

To avoid the problem of silica-based stationary phase/support instability one might limit oneself to mobile phases at moderate pH values.[3] This window of stability (perhaps pH 3–8) allows successful separation of a large number of analytes. However, many analytes, e.g., those with weakly acidic or basic moieties, benefit substantially from either very acidic or very basic mobile phases,[1] where these conditions set the protonation state of the analytes and stationary phase. A further need for stationary phase stability comes because chromatographic performance is often enhanced at higher temperatures, where mass transport of analytes is higher and solvent viscosity is lower. In summary, because of the limitations of silica, materials with improved pH stability have been and continue to be sought for in liquid chromatography.

A variety of approaches have been taken to increase the stability of silica-based stationary phases. For example, alkyl groups have been deliberately doped into SiO_2 during its fabrication to render it more resistant to hydrolysis, e.g., the XTerra columns by Waters (Milford, MA). Another approach has been to replace the methyl groups that were traditionally on monofunctional silane adsorbates with bulky side groups, e.g., isopropyl groups.[5] Although these approaches have extended

* To whom correspondence should be addressed.
[†] Brigham Young University.
[‡] U.S. Synthetic Corporation.
[§] Pacific Northwest National Laboratory.

(1) Snyder, L. R.; Kirkland, J. J.; Glajch, J. L. *Practical HPLC Method Development*, 2nd ed.; John Wiely: New York, 1997.
(2) Miller, J. M. *Chromatography: Concepts and Contrasts*, 2nd ed.; John Wiley & Sons, Inc.: Hoboken, NJ, 2005.
(3) Nawrocki, J.; Dunlap, C.; McCormick, A.; Carr, P. W. *J. Chromatogr., A* **2004**, *1028* (1), 1–30.
(4) Majors, R. E. *LCGC North Am.* **2008**, *26* (11), 1074–1090.
(5) Kirkland, J. J.; Glajch, J. L.; Farlee, R. D. *Anal. Chem.* **1989**, *61* (1), 2–11.

10.1021/ac1002068 © 2010 American Chemical Society
Published on Web 05/06/2010

the useful pH range of silica-based stationary phases, there is still room for improvement.

Another approach to this problem has been to replace silica with a more fundamentally stable material. For example, both porous graphitic carbon, e.g., the Hypercarb columns from Thermo Scientific,[6,7] and zirconia-based stationary phases, e.g., from ZirChrom, as well as alumina and titania, have been explored as possible LC stationary phases.[3,8] Zirconia has high chemical and thermal stability and can be used over a wide pH range.[9−11] It can be coated with polybutadiene to prepare a reversed-phase material;[12,13] however, Lewis acid sites on its surface lead to strong adsorption of certain species,[14−16] such as proteins,[12,13] and generally speaking, surface functionalization of zirconia has proved somewhat challenging.[8]

Diamond has also received some attention as a possible adsorbent for SPE and LC.[17] Diamond is remarkable; it is chemically inert, stable at both extremes of pH, and has high hardness, low compressibility, excellent optical transparency, and high thermal conductivity (ultimately, this may be important for eliminating thermal gradients in UPLC that affect separation efficiencies due to Joule heating).[18,19] Both our group and Nesterenko's have recently prepared and/or modified diamond as a substrate for SPE and/or LC. Nesterenko et al. performed normal phase high-performance liquid chromatography (HPLC) on microdispersed sintered detonation nanodiamonds (MSDNs).[20] They showed substantial improvements over previous attempts to use diamond in HPLC, i.e., they reported baseline separation of various compounds with 15 400 theoretical plates/m on *o*-xylene, although their peaks generally showed noticeable asymmetry (tailing), especially at longer retention times. In a related study, Purtov et al. developed a detonation nanodiamond−polysaccharide stationary phase for low-pressure (column) liquid chromatography.[21] Nesterenko et al. also used uncoated porous diamond materials derived from sintered detonation nanodiamonds for ion chromatography.[22]

Work in the Linford group at Brigham Young University (BYU) has focused on chemical modification of diamond. We first showed polyallylamine (PAAm)[23] adsorption from aqueous solution onto microdiamond and SPE of lipids on this amine-terminated diamond.[24] We then demonstrated that various alkyl and a perfluoroalkyl isocyanate would react with PAAm-terminated diamond.[25] An SPE extraction of pesticides from water could be performed on the resulting C_{18} material. In a different direction, we modified deuterium-terminated diamond powder with di-*tert*-amyl peroxide,[26] and also demonstrated its functionalization with polymers,[27] where the resulting modified diamond materials could again be used for SPE.

Two types of porous particles are commonly employed in LC today. The first, and more common, particle is completely porous. The second is pellicular and based on porous shells of material around solid cores (core−shell particles).[28] This latter approach benefits from faster mass transfer of analytes in and out of particles, which translates into an improvement in the "C term" of the Van Deemter equation, as evidenced by a flattening of the Van Deemter curve at higher mobile phase velocities.

Herein we explore the layer-by-layer (LbL) deposition of PAAm and nanodiamond on core particles to create high surface area particles for SPE and HPLC. In related work,[29,30] Ge and Chen coated SiO_2 core particles with a surfactant (sodium dodecyl sulfate, SDS), which could then be coated with TiO_2 particles, followed by SDS in an alternating fashion to produce core−shell particles.[31] The final step in their process was a sintering at 525 °C to burn out the SDS. Kirkland and Langlois reported the preparation of core−shell particles prepared on silica cores with silica/polyelectrolyte multilayers as shell layers. These particles were also heated to high temperature to remove the polyelectrolyte "glue".[32] In contrast, our substrate is diamond, not SiO_2, and we employ a mostly neutral polymer as the material that holds the particles together in the assembly—weak bases, such as amines, at the concentrations we employ, are mostly deprotonated (not charged) in water—a simple equilibrium calculation based on a 0.25 wt % aqueous solution of allyl amine (pK_b 4.31)[33] as a model compound for the PAAm polymer solution used to prepare the particles for HPLC indicates that ca. 3.3% of the amine groups on our PAAm polymer would be protonated (charged). This result justifies the use of a model compound for the polymer in this analysis because it indicates that the density of charged groups on the

(6) West, C.; Elfakir, C.; Lafosse, M. *J. Chromatogr., A*, in press.
(7) Pereira, L. *J. Liq. Chromatogr. Relat. Technol.* **2008**, *31* (11), 1687–1731.
(8) Nawrocki, J.; Dunlap, C.; Li, J.; Zhao, J.; McNeff, C. V.; McCormick, A.; Carr, P. W. *J. Chromatogr., A* **2004**, *1028* (1), 31–62.
(9) *Encyclopedia of Chromatography*; Cazes, J., Ed.; Marcel Dekker: New York, 2004; p 147.
(10) Nawrocki, J.; Rigney, M.; McCormick, A.; Carr, P. W. *J. Chromatogr., A* **1993**, *657* (2), 229–282.
(11) Rigney, M. P.; Weber, T. P.; Carr, P. W. *J. Chromatogr., A* **1989**, *484*, 273–291.
(12) Sun, L.; McCormick, A. V.; Carr, P. W. *J. Chromatogr., A* **1994**, *658* (2), 465–473.
(13) Sun, L.; Carr, P. W. *Anal. Chem.* **1995**, *67* (20), 3717–3721.
(14) Blackwell, J. *Chromatographia* **1993**, *35* (3), 133–138.
(15) Blackwell, J. A.; Carr, P. W. *J. Chromatogr., A* **1991**, *549*, 59–75.
(16) Blackwell, J. A.; Carr, P. W. *J. Liq. Chromatogr. Relat. Technol.* **1991**, *14* (15), 2875–2889.
(17) Nesterenko, P.; Haddad, P. *Anal. Bioanal. Chem.* **2010**, *396* (1), 205–211.
(18) Björkman, H.; Ericson, C.; Hjertén, S.; Hjort, K. *Sens. Actuators, B* **2001**, *79* (1), 71–77.
(19) Pierson, H. O. *Handbook of Carbon, Graphite, Diamond, and Fullerenes: Properties, Processing and Applications*; Noyes Publications: Park Ridge, NJ, 1993.
(20) Nesterenko, P. N.; Fedyanina, O. N.; Volgin, Y. V. *Analyst* **2007**, (132), 403–405.
(21) Purtov, K.; Puzyr', A.; Bondar', V. *Dokl. Biochem. Biophys.* **2008**, *419* (1), 72–74.
(22) Nesterenko, P. N.; Fedyanina, O. N.; Volgin, Y. V.; Jones, P. *J. Chromatogr., A* **2007**, *1155* (1), 2–7.
(23) Saini, G.; Gates, R.; Asplund, M. C.; Blair, S.; Attavar, S.; Linford, M. R. *Lab Chip* **2009**, *9* (12), 1789–1796.
(24) Saini, G.; Yang, L.; Lee, M. L.; Dadson, A.; Vail, M. A.; Linford, M. R. *Anal. Chem.* **2008**, *80* (16), 6253–6259.
(25) Saini, G.; Wiest, L. A.; Herbert, D.; Biggs, K. N.; Dadson, A.; Vail, M. A.; Linford, M. R. *J. Chromatogr., A* **2009**, *1216* (16), 3587–3593.
(26) Yang, L.; Lua, Y.-Y.; Tan, M.; Scherman, O. A.; Grubbs, R. H.; Harb, J. N.; Davis, R. C.; Linford, M. R. *Chem. Mater.* **2007**, *19* (7), 1671–1678.
(27) Yang, L. Functionalization, Characterization, and Applications of Diamond Particles, Modification of Planar Silicon, and Chemometrics Analysis of Mass Spectrometry Data. Brigham Young University, Provo, UT, 2009.
(28) Kirkland, J. J.; Landlois, T. J.; DeStefano, J. J. *Am. Lab.* **2007**, *8* (39), 18–20.
(29) Lvov, Y. M.; Price, R. R. *Colloids Surf., B* **2002**, *23* (4), 251–256.
(30) Caruso, F.; Fiedler, H.; Haage, K. *Colloids Surf., A* **2000**, *169* (1−3), 287–293.
(31) Ge, J.; Li, Y.; Chen, L. *J. Liq. Chromatogr. Relat. Technol.* **2006**, *29* (16), 2329–2339.
(32) Kirkland, J. J.; Langlois, T. J. U.S. Patent 2007/0189944A1, 2007.
(33) *Lange's Handbook of Chemistry*, 15th ed.; McGraw-Hill Handbooks, 1999.

Scheme 1. Synthesis of Core–Shell Particles[a]

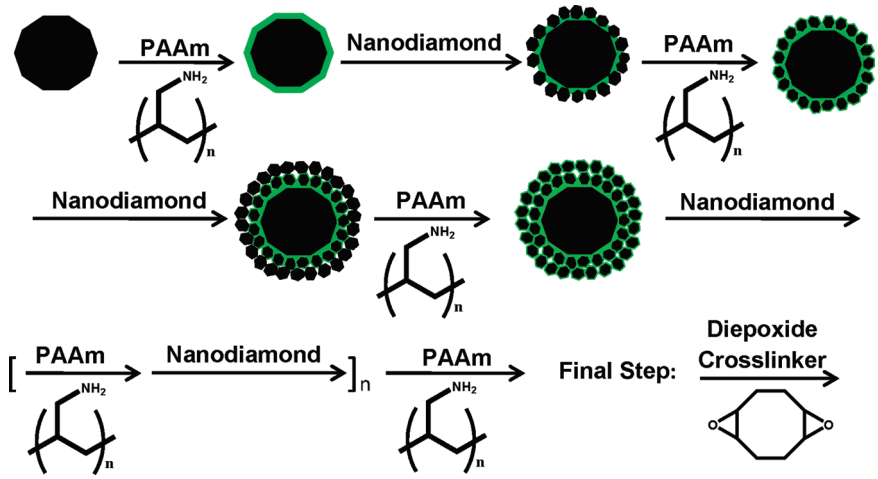

[a] The actual PAAm–nanodiamond shells are porous and somewhat irregularly shaped.

polymer will be low. The PAAm polymer is not removed by heating after formation of the particles. That this polymer remains is an advantage because it allows subsequent stationary phase creation through reactive primary amine groups. This work also differs from our earlier studies in which we used low surface area, nonporous particles.[24,25,27,34]

Particle preparation is shown in Scheme 1. First, PAAm adsorbs from aqueous solution onto core diamond particles. These PAAm-terminated core particles are then immersed in a suspension of nanodiamond particles, which adsorb onto the PAAm-coated particles. This process is repeated in an alternating fashion. Finally, the particles are reacted with a cross-linker (1,2,5,6-diepoxycyclooctane) and/or a long-chain epoxide (1,2-epoxyoctadecane). The resulting core–shell particles have significantly more surface area than the original solid particles. Larger, ca. 50 μm, particles are used for SPE, and smaller, ca. 3 μm, particles are used for HPLC. To the best of our knowledge HPLC separations with these core–shell diamond particles now show the highest efficiencies yet reported for a diamond-based chromatographic support.

EXPERIMENTAL SECTION

Reagents. Poly(allylamine) (PAAm) (M_w ca. 65 000 or 17 000, 20 wt % solutions in water, Aldrich, Milwaukee, WI), 1,2,5,6-diepoxycyclooctane (96%, Aldrich), 1,2-epoxyoctadecane (90%, Alfa Aesar, Ward Hill, MA), and 1,16-hexadecanedioic acid (≥98%, Aldrich) were used as received. Monocrystalline diamond powders (1.7, 5, and 50–70 μm and 10–50 and 100–250 nm), which had been crushed and sized, were obtained from Advanced Abrasives (Tennsauken, NJ). The 10–50 nm nanodiamond particles were obtained as a stable, aqueous suspension and used as received. The 100–250 nm diamond powder was obtained as a dry material and used as received—it did not appear opportune to clean it because of its small size. Silicon wafers (test grade, n-type, ⟨1–0–0⟩ orientation, 2–6 Ω·cm) were purchased from UniSil Corporation, California.

Deposition of PAAm–Nanodiamond Bilayers on Si/SiO_2. Native oxide-terminated silicon wafers were cleaved into ca. 1.5 × 1.5 cm pieces, cleaned with a 2 wt % sodium dodecyl sulfate solution in water using a camel hair brush, and then rinsed thoroughly with deionized water. These clean substrates were cleaned with an air plasma for 1 min in a plasma cleaner (model PDC-32G from Harrick Plasma (Ithaca, NY) on its high power setting—16 W applied to the rf coil), immersed in an aqueous solution of PAAm (0.25 wt %, M_w 65 000) for 5 min, and removed and rinsed thoroughly with deionized water. The resulting PAAm-coated surfaces were then immersed in an aqueous suspension of 250 nm nanodiamond (1.0 wt %) for 5 min. The surface was rinsed thoroughly with deionized water to remove nonspecifically adsorbed nanodiamond particles. This led to the formation of the first bilayer of PAAm–nanodiamond on the surface. Surfaces containing two, three, four, five, and nine bilayers were similarly made by alternating immersions in the PAAm solution and nanodiamond suspension.

Synthesis of Core–Shell Particles for SPE. Core–shell particles for SPE were synthesized from 50–70 μm (core) and 100–250 nm (shell) diamond particles. Prior to PAAm deposition, the microdiamond was cleaned in piranha solution (70% H_2SO_4 (concd)/30% H_2O_2 (concd)) at 100 °C for 1 h, sonicated in ultrapure water, and washed extensively with ultrapure water on a filter funnel.

Core–shell particles containing zero to five and nine bilayers of PAAm–nanodiamond were synthesized. A 0.25 wt % solution of poly(allylamine) was made from 1.55 g of a solution of PAAm (M_w 65 000, 20 wt % solution) in 125 mL of ultrapure water, and 12 g of piranha-cleaned microdiamond powder was poured into this solution. The solution was shaken for ca. 10 s every 10 min for 1 h to fully expose the particles to PAAm. The diamond powder was then washed extensively with ultrapure water on a filter funnel. An aqueous suspension of 100–250 nm nanodiamond powder was prepared by sonicating 1 g of nanodiamond in 120 mL of ultrapure water, and 12 g of PAAm-functionalized microdiamond powder was poured into this suspension for 1 h. This suspension was again shaken gently for ca. 10 s every 10 min to expose all surfaces of the coated microdiamond particles to nanodia-

(34) Yang, L.; Vail, M. A.; Dadson, A.; Lee, M. L.; Asplund, M. C.; Linford, M. R. *Chem. Mater.* **2009**, *21* (19), 4359–4365.

mond particles. The aqueous suspension was then filtered on a medium pore size (25−50 μm) filter funnel. As the size of the nanodiamond particles is much smaller than the pore size of the filter funnel, loose nanodiamond particles in the suspension easily passed through the pores of the filter funnel leaving microdiamonds coated with nanodiamond particles; these particles were washed extensively with ultrapure water on the filter funnel to remove any weakly adsorbed or unbound nanodiamonds. Approximately 2.8 g of these coated microdiamonds were then taken for characterization, and the remainder was poured into the next aqueous solution of PAAm for 1 h to amine functionalize the outer surface of the nanodiamonds particles in the first layer. The cleaning procedure was repeated as before. This powder was then poured into an aqueous suspension of nanodiamonds as in the first deposition of nanodiamond. Another 2.8 g of this functionalized diamond powder was taken, and the remainder was modified with more PAAm and nanodiamond. This general procedure was repeated until the desired number of PAAm−nanodiamond bilayers was deposited.

Chemical Cross-Linking of Core−Shell Particles. The mechanical stability of core−shell particles is expected to be somewhat low because nanodiamond particles, microdiamond particles, and adsorbed PAAm are most likely held together through noncovalent interactions. The mechanical stability of these particles was improved by chemical cross-linking with 1,2,5,6-diepoxycyclooctane. To wit, ca. 2.6 g of each of the different core−shell particles was crossed-linked with a 2.3 wt % solution of 1,2,5,6-diepoxycyclooctane (0.175 g of the diepoxide dissolved in 7.5 mL of isopropyl alcohol). The reaction was performed in a sealed, thick-walled glass reaction vessel at 80 °C overnight. After the reaction, the core−shell diamond powder was washed extensively on a filter funnel with copious quantities of isopropyl alcohol, followed by dichloromethane.

Surface Analysis. FT-IR was performed with a Magna-IR 560 spectrometer from Nicolet (Madison, WI). Environmental scanning electron microscopy (ESEM) images of the samples were acquired using an FEI (Philips) XL30 ESEM FEG instrument. Since diamond is an insulator, the diamond powder was adhered to a conductive, double-sticky carbon tape, and the ESEM FEG instrument was operated in low-vacuum mode to prevent surface charging. Samples were sent to Micromeritics (Norcross, GA) for surface area (BET) and pore size analysis. Rutherford backscattering (RBS) and nuclear reaction analysis (NRA) were performed at EMSL, Environmental Molecular Sciences Laboratory, at the Pacific Northwest National Laboratory. RBS measurements were performed with 2.0 MeV He^+ ions, and the backscattered He^+ ions from the sample were collected using a surface barrier detector positioned at a scattering angle of 165°. NRA measurements were performed using 0.94 MeV D^+ ions. The $^{12}C(d,p)^{13}C$ nuclear reaction was used to measure the total amount of C in the samples and was calibrated with a 500 Å carbon standard that contains 568×10^{15} carbon atoms/cm^2. A surface barrier detector at the scattering angle of 170° was used to collect the protons generated from the nuclear reaction. An aluminized Mylar foil was positioned in front of the detector to block the backscattered D^+ ions from entering the detector.

Solid-Phase Extraction. The analyte used to determine breakthrough volumes was 1,16-hexadecanedioic acid in 3:1 $CHCl_3$/isopropyl alcohol (IPA). The column was first conditioned with six column volumes of 0.5 NH_4OH to deprotonate any protonated amines, and then washed with three column volumes each of IPA, 50% IPA/50% hexane, and hexane. After conditioning, the analyte was loaded onto the cartridge. The column was maintained wet, and the flow rate was constant throughout the process. Equal volumes of the fractions eluting from the column were collected in individual vials. Lastly, each individual fraction was analyzed by electrospray ionization mass spectrometry (ESI-MS) (Agilent LC/MSD TOF model no. G1969A).

Synthesis of Core−Shell Particles for HPLC. Core−shell particles for HPLC were synthesized from 1.7 μm diamond core and 10−50 nm diamond particles. Particles were made in a 50 mL screw cap plastic tube. An aqueous suspension of 2.4 g of 1.7 μm diamond particles was prepared in the screw cap tube (total solution volume ca. 45 mL), and 250 μL of 7.5 wt % aqueous solution of PAAm (17 000 M_w) was added to it. The tube was then shaken for 3 min to homogeneously expose the particles to PAAm. After treatment with PAAm solution, the tube was centrifuged at 5000 rpm for 2 min. The supernatant was decanted, and the settled particles were washed twice with 45 mL of deionized water. An aqueous suspension of these particles was then made, and 1 mL of an 8.3 wt % aqueous suspension of 10−50 nm diamond was added to it. The tube was shaken for 3 min to expose the PAAm-functionalized diamond particles to the nanodiamond particles. After this treatment, the tube was again centrifuged for 2 min at 5000 rpm. The supernatant was decanted and the particles were washed twice with 45 mL of deionized water. This alternating treatment with PAAm and nanodiamond was continued until the desired number of PAAm−nanodiamond bilayers was formed.

HPLC Column Packing. Core−shell particles were packed in a 30 mm × 4.6 mm column using a Chrom Tech (Apple Valley, MN) packing system. A slurry of these particles was prepared in 50:50 acetone/water. Column packing was done at a constant flow 0.8 mL/min for 25 min.

Cross-Linking of Core−Shell Particles for HPLC. Core−shell particles were chemically cross-linked with a 0.38 wt % solution of 1,2,5,6-diepoxycyclootane in xylenes and cyclohexanol (6.7:1) (v/v) mixture. The reaction was done overnight under nitrogen at 130 °C. The particles were then washed extensively with xylenes and then isopropyl alcohol.

Functionalization of Core−Shell Particles with C_{18} Groups. A 1.7 wt % solution of 1,2-epoxyoctadecane (made in a 6.7:1 xylene/cyclohexanol mixture) was used to attach C_{18} chains to core−shell particles that had not previously been cross-linked. The reaction was done overnight in a nitrogen atmosphere at 130 °C. After the reaction, the particles were washed extensively with xylene and then isopropyl alcohol.

HPLC on Core−Shell Particles. A Waters 1525 HPLC system was employed with an absorbance detector set at 254 nm. The instrument software (Breeze version 3.30 SPA) was used to calculate retention factors (k), numbers of theoretical plates per meter (N/m), and asymmetry factors. (The software calculated

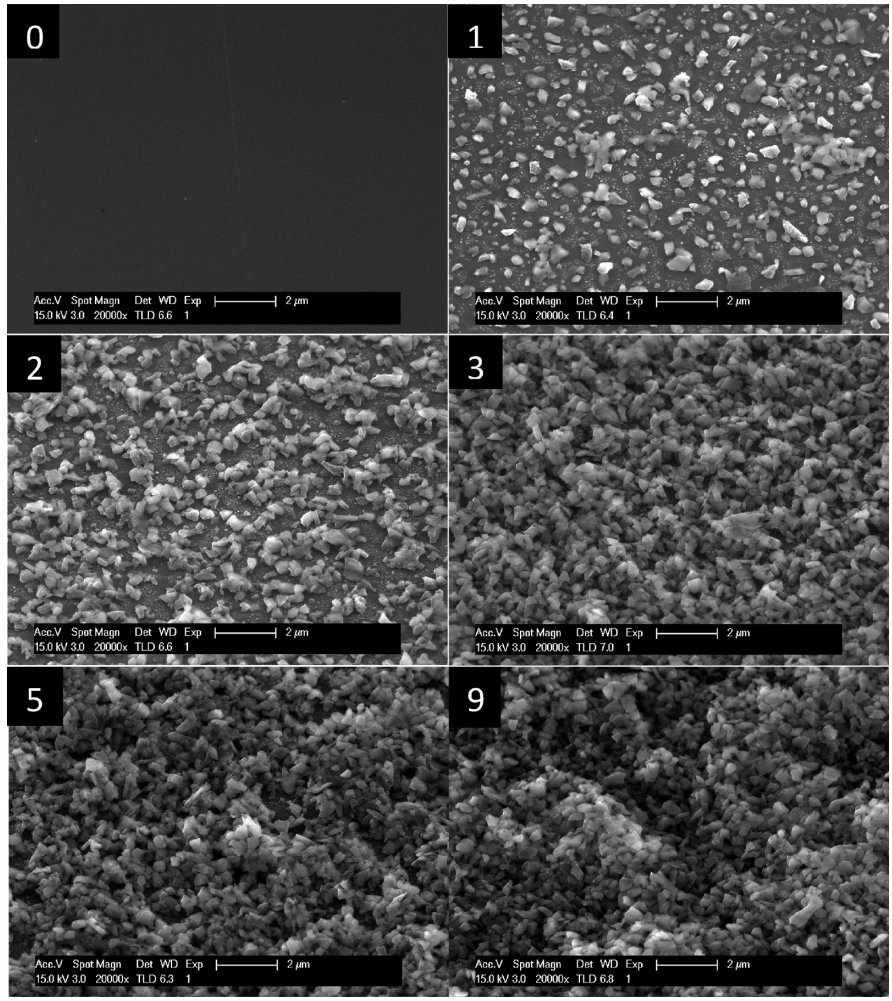

Figure 1. SEM images of silicon surfaces containing various numbers of PAAm−nanodiamond (100−250 nm) bilayers: zero, one, two, three, five, and nine.

the number of theoretical plates at full width at half-maximum for all the chromatographic peaks.) Core−shell particles cross-linked with 1,2,5,6-diepoxycyclooctane were employed as a normal phase to separate benzophenone and dinitrobenzene. The mobile phase was 70:30 hexanes/ethylacetate (each solvent contained 0.2% (v/v) triethylamine). The flow rate was 0.3 mL/min. C_{18}-functionalized core−shell particles were used as a reversed phase to separate cyanazine and diazinon, and also a mixture of benzene, toluene, xylene and mesitylene. The mobile phase composition was 50% acetonitrile and 50% water (each solvent contained 0.1% (v/v) triethylamine). The flow rate was 0.2 mL/min.

RESULTS AND DISCUSSION

Core−Shell Diamond Particles for Solid-Phase Extraction. LbL deposition of PAAm and nanodiamond on planar Si/SiO_2 was studied by scanning electron microscopy (SEM), RBS, and NRA. RBS and NRA are well-suited as analytical techniques for these surfaces because of the high energies (deep surface penetrations) of their incident and scattered/created particles. Figure 1 shows SEM images of the silicon surfaces containing zero, one, two, three, five, and nine bilayers of PAAm−nanodiamond. As is evident, the surface is not fully covered by nanodiamond after the deposition of one bilayer, as bare silicon is still visible in some regions. But with an increase in the number of PAAm−nanodiamond bilayers, the number density of nanodiamond particles at the surface increases with a concomitant disappearance of the underlying silicon surface. Figure 2 shows the RBS spectra of the surfaces containing zero, one, three, five, and nine bilayers of PAAm−nanodiamond. The spectra show the silicon and/or carbon edges that originate from the silicon substrate and/or the carbon in the nanodiamond and obviously to a lesser degree from PAAm. The RBS spectrum of the surface containing no bilayer is dominated by the silicon edge. In the spectrum of the surface containing one bilayer, a small peak due to C appears, which confirms the deposition of PAAm and nanodiamond on the surface. In addition, the peak due to Si decreases in intensity around its edge, although a significant fraction (ca. 50%) of the edge remains, which is consistent with the partial coverage of the silicon substrate by one bilayer shown by SEM in Figure 1. As the number of PAAm−nanodiamond bilayers increases, the step height of C at its edge increases due to an increase in the amount of carbon on the surface, and the signal due to unattenuated silicon at its edge decreases. For the surface containing nine bilayers of PAAm−nanodiamond, it is significant that the Si edge

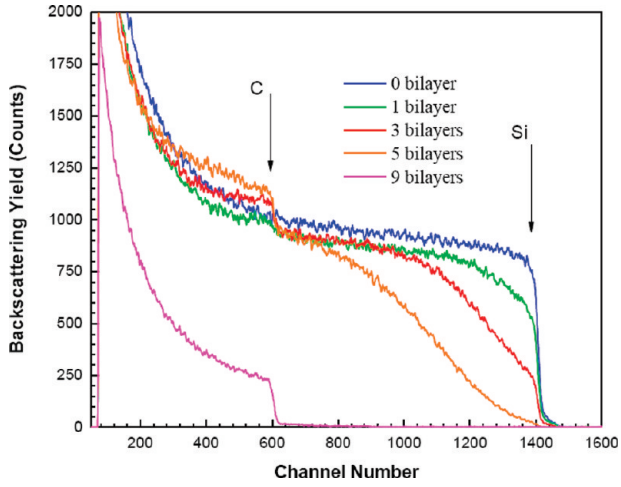

Figure 2. RBS spectra of silicon surfaces containing zero, one, two, three, five, and nine bilayers of PAAm−nanodiamond (100−250 nm).

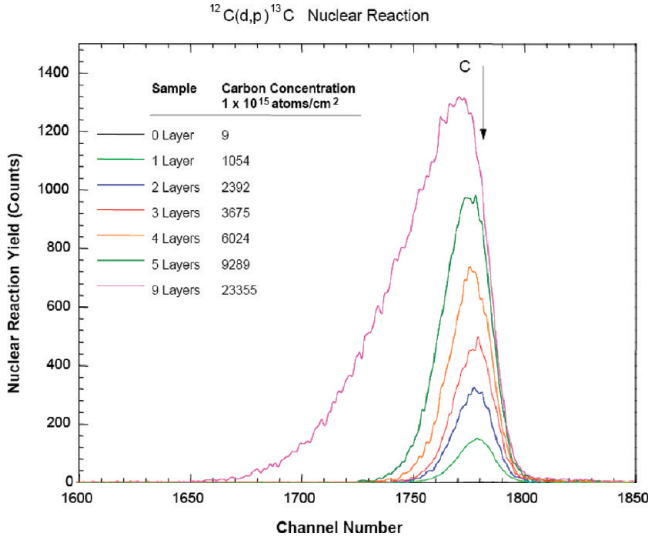

Figure 3. NRA spectra of silicon surfaces containing zero, one, two, three, five, and nine bilayers of PAAm−nanodiamond (100−250 nm).

has disappeared (it is fully attenuated), leaving only the C edge at its maximum intensity.

Figure 3 shows the carbon signal, along with the number of carbon atoms/cm^2, from NRA of surfaces containing different numbers of PAAm−nanodiamond bilayers. In this NRA analysis, energetic deuterons fuse with ^{12}C nuclei and eject energetic protons: (^{12}C(d,p)^{13}C, i.e., $^{12}C + {}^{2}H \rightarrow {}^{1}H + {}^{13}C$). The carbon signal increases steadily with an increase in the number of PAAm−nanodiamond bilayers, which further reinforces the observations derived from the SEM and RBS data. The significant tailing of the nine-bilayer sample is a result of attenuation of the protons in the thicker multilayer film. It is significant that the NRA signal provides absolute quantization of the total carbon content (atoms/cm^2) at the silicon surface.

In the synthesis of core−shell particles, the LbL deposition of nanodiamond particles around a solid microdiamond core was monitored by four techniques: diffuse reflectance Fourier transform infrared spectroscopy (DRIFT), ESEM, Brunauer−Emmett−Teller (BET) surface area measurements, and sorbent (analyte)

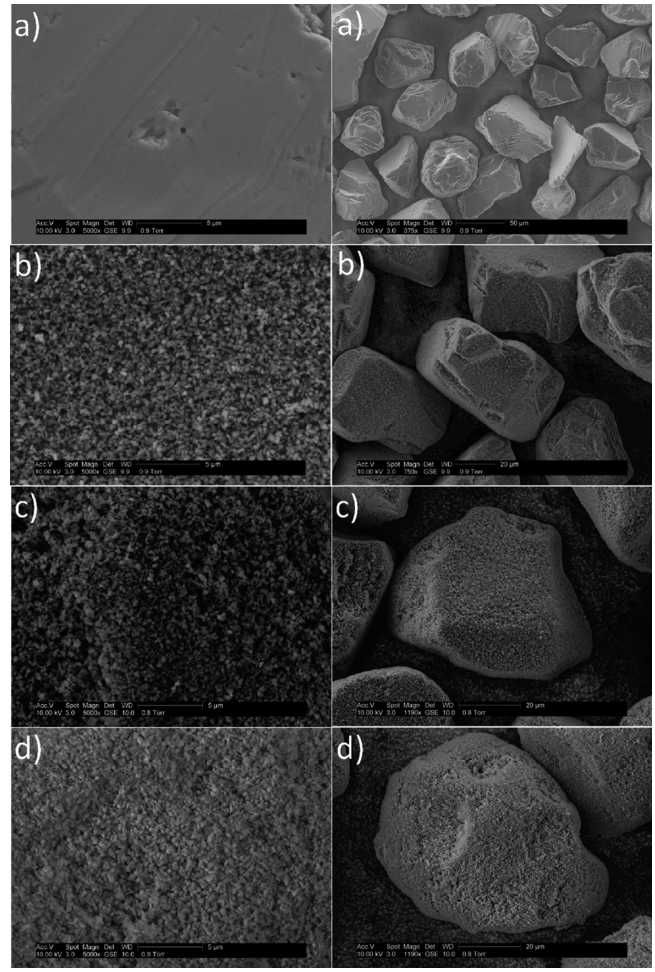

Figure 4. ESEM images of 50−70 μm diamond particles containing (a) zero, (b) three, (c) five, and (d) nine bilayers of PAAm−nanodiamond (100−250 nm).

capacity measurements obtained during solid-phase extraction. Figure 4 shows ESEM images of micrometer-sized core−shell diamond particles containing zero, three, five, and nine bilayers of PAAm−nanodiamond. As was the case for the planar surfaces, it is clear that nanodiamond particles begin to adsorb onto the surface of PAAm-functionalized microdiamonds after their first immersion in an aqueous suspension of nanodiamonds. ESEM shows that with an increase in the number of nanodiamond layers, the surface becomes fuzzier in appearance, suggesting higher porosity. Core−shell particles were also characterized by DRIFT. Figure 5 shows a plot of the area of the C−H stretching region of the core−shell particles as a function of the number of PAAm−nanodiamond bilayers. It is evident that the area of the C−H stretching region increases with an increase in the number of bilayers where this increase is attributed to C−H stretches in the PAAm polymer. The fact that the surface area, C−H stretching area, and analyte capacity do not increase linearly with number of PAAm−nanodiamond bilayers in Figure 5 may be attributable to the well-known "induction period" in LbL deposition—often, a few layers must be deposited before the system begins to show linear increases.[35,36] Two other effects that may also contribute to this lack of linearity may be the increasing radii of the

(35) Schuetz, P.; Caruso, F. *Colloids Surf., A* **2002**, *207* (1−3), 33−40.

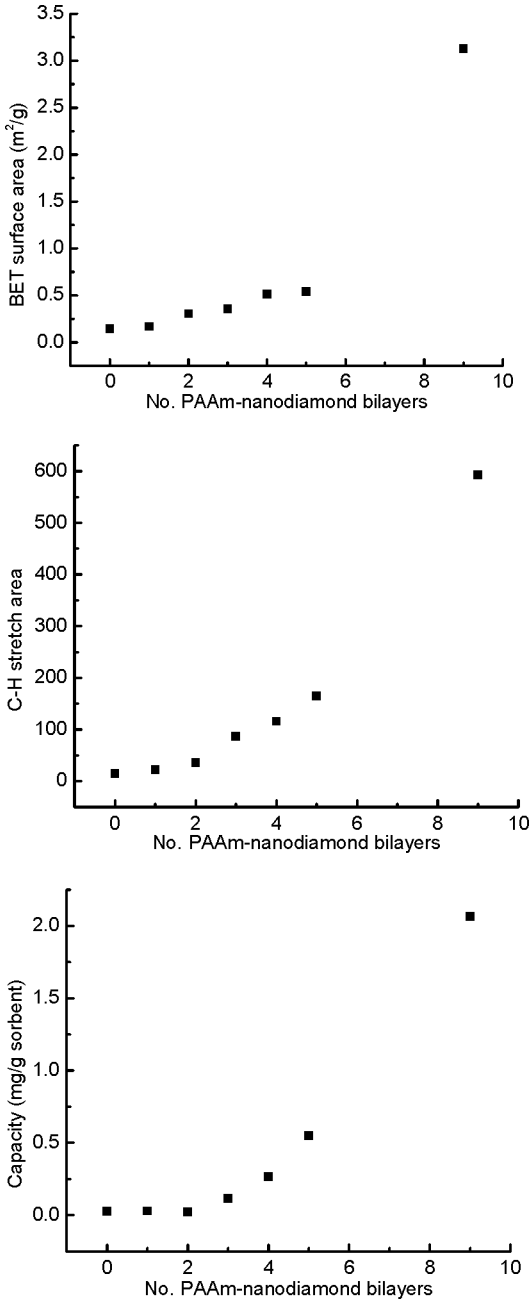

Figure 5. Plots of the area of the C−H stretching region, BET surface area, and analyte capacity vs number of PAAm−nanodiamond (100−250 nm) bilayers on 50−70 μm core diamond particles.

particles and the increase in surface roughness, and therefore area of the outermost surface, suggested in the ESEM images shown herein.

The primary objective of this work was to synthesize porous diamond powder with high surface areas; we believed that the deposition of multilayers of nanodiamond particles around a solid microdiamond core would make the structure porous, and increase its surface area. Figure 5 shows a plot of the BET surface area of the core−shell particles versus the number of PAAm−nanodiamond bilayers. As expected, with an increase in the number of nanodiamond layers, the structure becomes more porous.

(36) Caruso, F.; Niikura, K.; Furlong, D. N.; Okahata, Y. *Langmuir* **1997**, *13* (13), 3422–3426.

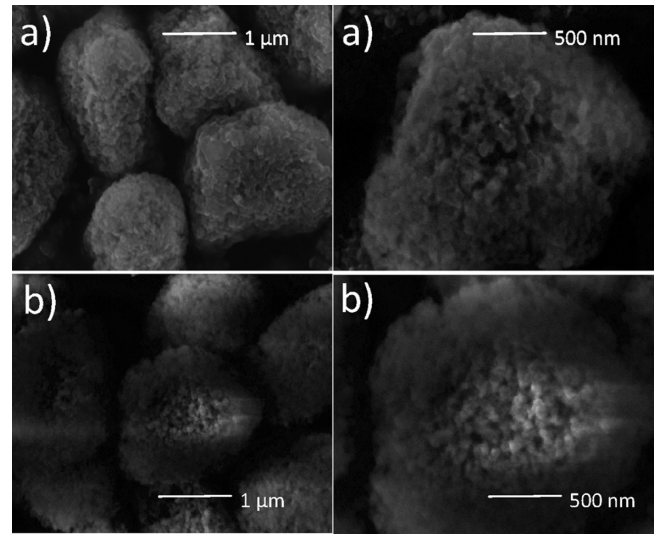

Figure 6. ESEM images of (a) 14 and (b) 28 PAAm−nanodiamond (10−50 nm) bilayers on ca. 1.7 μm diamond cores.

Table 1. Core−Shell Diamond Particles Produced with Bilayers of 10−50 nm Nanodiamond and PAAm[a]

core size (μm)	no. of bilayers	BET surface area (m^2/g)	average pore size (nm)
5	13	6.8	25.9
1.7	14	19.4	
1.7	28	30.3	20.4

[a] Note that diamond is ca. 2× as dense as silica, so these surface area numbers should be multiplied by ca. 2 to put them on equal footing with silica.

The average pore size of the core−shell particles containing nine layers of nanodiamond particles was 134 Å by the BET method.

As further characterization, the SPE capacity of the core−shell particles was determined. Figure 5 contains a plot of the capacity of the core−shell particles versus the number of nanodiamond layers. As expected, the analyte capacity increases with an increase in the surface area. For core−shell particles containing nine layers of nanodiamond particles a ca. 80-fold increase in capacity was observed compared to solid, nonporous diamond powder.

Core−Shell Diamond Particles for HPLC. The general LbL strategy outlined above for making diamond-based particles for SPE could also be applied to create particles for HPLC, where now the core and shell particles were ca. 1.7 or 5 μm and 10−50 nm, respectively. Figure 6 shows ESEM images of such particles with 14 and 28 bilayers of PAAm and nanodiamond. These particles showed much higher surface areas than those made for SPE (see Table 1). For example, 13 bilayers of PAAm−nanodiamond on 5 μm core diamond particles produced materials with ca. 7 m^2/g of surface area. (Note that diamond is about twice as dense as silica, so surface areas per gram of diamond particles should be multiplied by 2 if they are to be compared directly to surface areas per gram of silica particles.) As expected, when the size of the core particle shrinks, the surface area of the particles increases. For example, 1.7 μm cores particles with 14 and 28 PAAm−nanodiamond bilayers have 19 and 30 m^2/g of surface

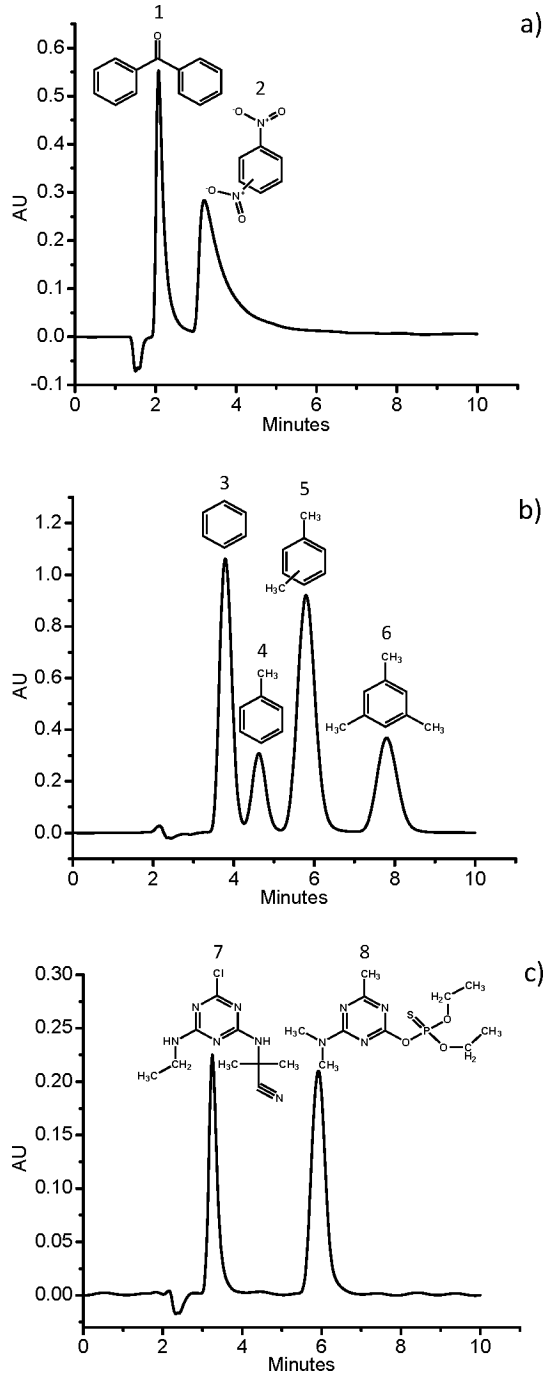

Figure 7. (a) Normal phase separation of benzophenone and nitrobenzene with a mobile phase composition of 70% hexane and 30% ethyl acetate (each containing 0.2% triethylamine). The flow rate was 0.3 mL/min. (b) Reversed-phase C_{18} separation of benzene, toluene, xylene, and mesitylene with a mobile phase composition of 50% acetonitrile and 50% water (each solvent had 0.1% triethylamine in it). The flow rate was 0.2 mL/min. (c) Reversed-phase C_{18} separation of two pesticides (cyanazine and diazinon) with a mobile phase composition of 50% acetonitrile and 50% water (each solvent contained 0.1% triethylamine).

area, respectively (again these numbers should be multiplied by 2 if they are to be compared with silica).

As with the particles prepared for SPE above, the 28 bilayer particles were cross-linked with 1,2,5,6-diepoxycyclooctane to create a mixed mode stationary phase containing amino, hydroxyl, and cyclooctyl groups that would be expected to also have a strong normal phase character. These particles were packed in a 4.6 mm × 30 mm column, and benzophenone and dinitrobenzene could be separated, where the dinitrobenzene showed significant tailing (see Figure 7 and Table 2). Nevertheless, this column showed good stability. Essentially no change in column performance was observed after the mobile phase (33:67 ethyl acetate/hexane with 0.2% TEA) was pumped through the column at 0.3 mL/min for 15.5 h (see the Supporting Information).

Table 2. Retention Factors (*k*), Plates per Meter (N/m), and Asymmetries for Compounds Separated by HPLC on Normal Phase and Reversed-Phase Diamond Core−Shell Particles

		k	N/m	asymmetry
1	benzophenone[a]	0.521	22 800	2.631
2	1,4-dinitrobenzene[a]	1.355	5720	5.184
3	benzene[b]	0.760	22 800	1.103
4	toluene[b]	1.146	27 700	n/a
5	xylene[b]	1.691	26 300	1.089
6	mesitylene[b]	2.620	36 300	1.074
7	cyanazine[b]	0.511	40 000	1.260
8	diazinon[b]	1.760	54 800	1.034

[a] Normal-phase. [b] Reversed-phase.

Although of course amino and/or mixed mode phases are of importance in HPLC, most separations are performed on C_{18} columns. Accordingly, 28 layer PAAm−nanodiamond particles were treated with 1,2-epoxyoctadecane to make a C_{18} phase, where, as before, the carbon−nitrogen bonds formed during oxirane ring-opening are highly resistant to hydrolysis under either acidic or basic conditions. Separations showing good symmetry of peaks were performed on the resulting HPLC column (see Figure 7 and Table 2). That is, nearly baseline separation of a series of alkyl benzenes was obtained, and baseline separation of two pesticides was also demonstrated. The alkylbenzenes separated in Figure 7 show ca. 22 800, 27 700, 26 300, and 36 300 plates/m for benzene, toluene, xylene (more than one isomer in the sample mixture), and mesitylene, respectively. Even more impressive was a separation of two pesticides (cyanazine and diazinon), which showed 40 000 and 54 800 plates/m, respectively. To the best of our knowledge, these results show the highest number of plates per meter that have been reported for any diamond-based LC column.

Unfortunately, columns packed with these C_{18} particles were not as stable as those made by cross-linking with the diepoxide; degradation in the column was observed after mobile phase was pumped through it overnight. Taken together, these results of the mixed mode and C_{18} materials suggest that our general strategy for preparing core−shell particles can produce stable stationary phases for HPLC—future work will focus on cross-linking the particles, after which they will be modified to form C_{18} phases.

CONCLUSION

We have reported the formation of porous core−shell diamond particles for SPE and HPLC. The effect of LbL deposition of nanodiamond particles on various parameters such as surface area, analyte capacity, IR absorption, etc., was determined. Core−shell

diamond particles have higher surface areas and capacities than solid diamond particles, where these properties increase with the number of PAAm−nanodiamond bilayers. HPLC separations with relatively high numbers of plates per meter were demonstrated on C_{18} phases.

ACKNOWLEDGMENT

This work was supported by U.S. Synthetic Corporation, Orem, UT. Part of this research was performed at EMSL, a national scientific user facility sponsored by the Department of Energy's Office of Biological and Environmental Research and located at Pacific Northwest National Laboratory.

SUPPORTING INFORMATION AVAILABLE

Additional information related to the stability of the normal phase column. This material is available free of charge via the Internet at http://pubs.acs.org.

Received for review January 24, 2010. Accepted April 21, 2010.

AC1002068